Available online at www.sciencedirect.com

ScienceDirect

Energy Procedia 00 (2013) 000–000

Energy Procedia

www.elsevier.com/locate/procedia

PV Asia Pacific Conference 2012

Continued Development of All-Back-Contact Silicon Wafer Solar Cells at ANU

Ngwe Zin[a,*], Andrew Blakers[a], Keith R. McIntosh[b], Evan Franklin[a], Teng Kho[a], Kean Chern[a], Johnson Wong[c], Thomas Mueller[c], Armin G. Aberle[c], Yang Yang[d], Xueling Zhang[d], Zhiqiang Feng[d], Qiang Huang[d], Pierre J. Verlinden[d]

[a]*Australian National University, Canberra, ACT 0200, Australia*
[b]*PV Lighthouse, Wollongong NSW 2500, Australia*
[c]*Solar Energy Research Institute of Singapore, National University of Singapore, 7 Engineering Drive 1, Block E3A, Singapore 117574, Singapore*
[d]*State Key Lab of PV Science and Technology, Trina Solar Limited, No. 2 Trina Road, Trina PV Park, New District, Changzhou, Jiangsu, China 213031 China*

Abstract

The collaboration between the Solar Energy Research Institute of Singapore (SERIS), Trina Solar and ANU is progressing well, and ANU has already developed all-back-contacted (ABC) silicon wafer cells with best one-sun efficiencies of 21.2% and 22.1% on FZ material, when measured with the aperture areas of 16 cm^2 (includes busbars) and 13 cm^2 (excludes busbars) respectively. This paper presents the continuing development of ABC cells targeting the efficiency of 23.5% on 16-cm^2 cell area. Further developments such as optimising front surface field (FSF), rear diffusion, anti-reflection coating (ARC), and incorporation of lithographically aligned metal contacts were undertaken on the ABC cells. Phosphorus diffusion of the FSF was made lighter from the sheet resistance of 190 Ω/□ to 240 Ω/□, resulting in the reduction of the saturation current density (J_{oe}) of the FSF by 22 fA/cm^2. The optimised thickness of anti-reflection coating (ARC) PECVD SiN_x further reduces the average reflectance across the wavelength range of 300 to 1200 nm by about 4%. Incorporation of aligned metal contacts and heavier rear phosphorus diffusion has contributed to the reduction in the total series resistance by 0.08 Ωcm^2. The above optimised improvements have increased the efficiency of the champion ABC cell by 0.5% absolute. In addition, we present further refinements in areas of texturing; FSF passivation; electrical shading loss in terms of cell pitch, bus-bar and base doping; and metallisation to aim for the 16-cm^2 ABC cells with the conversion efficiency > 22% in the near term.

Keywords: back-contact; FSF; electrical shading loss; photoconductance; OPAL 2; PC2D

* Corresponding author. Tel.: +612 6125 7450; fax: +612 6125 8873
E-mail address: soe.zin@anu.edu.au

1. Introduction

In 2010, the leading PV manufacturer Trina Solar and the Solar Energy Research Institute of Singapore (SERIS) signed a research agreement to develop high-efficiency ABC silicon wafer solar cells. The research agreement targets to realise up to 21.5% production efficiency, and up to 23.5% laboratory test efficiency [1]. The involvement of the Australian National University (ANU) in the project is to develop laboratory-sized (16-cm^2) ABC silicon solar cells on n-type wafer substrates, targeting to an efficiency of 23.5% within two years of project commencement.

The quest of the research collaboration between Trina Solar, SERIS, and ANU to develop high-efficiency ABC silicon wafer solar cells is driven by the fact that the cost of the silicon wafer material is still significant in a photovoltaic module, and the photovoltaic industry is always in search of thinner wafer and different solar cell manufacturing technique, with the aim of further driving down the cost of photovoltaic module. Rear contact solar cells offer the opportunity to increase cell efficiency. Key advantages associated with the ABC solar cell design involve no optical shading loss with front metal grid, independent optimisation of surface passivation and optics at the front, large metal coverage on the rear that minimises series resistance, improved rear optics, simpler cell interconnecting system, and ease of adopting n-type Si, which is resilient to metal and oxygen impurities.

Schwartz and Lammert of Purdue University first proposed the ABC cell structure for concentrator applications [2, 3]. Research on ABC cells was further carried out by Sandia [4, 5] and Stanford University [6, 7]. SunPower was then established in 1985 to commercialise the Stanford developed technology. In 2010 SunPower reported remarkable efficiencies of large-area solar cells (155.1 cm^2) of up to 24.2% in a commercial production environment [8, 9].

At ANU, since the project commenced in March 2011, ABC silicon solar cells made from FZ wafers with encouraging conversion efficiencies of 19% (16-cm^2), 21.2% (16-cm^2) and 22.1% (13-cm^2) have been developed, and the results of which have been published elsewhere [10-12]. Table 1 shows the one-sun electrical parameters of 16-cm^2 (which includes busbars) ABC cell [12]. In this publication, we analysed the improvement items – optimisation of FSF, ARC, rear diffusion and aligned metal contacts – that were incorporated in the current process. In the analysis, the results of current process on further optimisations will be compared against that of the old process, described elsewhere [12]. Besides, we present the results of further refinements to incorporate in the next cell processes. Refinements include improved texturing; advanced passivation; minimising electrical shading loss in terms of substrate resistivity, busbar geometry and device pitch (i.e. n- to p-diffusion); and improved metallisation scheme.
We use photoconductance (PC) technique to analyse the performance of passivation and extraction of saturation current density (J_{oe}); spectral response analysis to determine the front surface reflectance; OPAL 2 to analyse the performance of anti-reflection layer and texture condition [13], and PC2D to model the performance of ABC cells based on different pitches and substrate resistivity [14].

Table 1. One-sun electrical parameters of ABC cells measured using 16-cm^2 aperture mask, published elsewhere [12].

Cell	Voltage	Jsc (mA/cm2)	FF	Efficiency
14.5B	0.684	39.0	0.794	21.2
14.5A	0.682	38.3	0.794	20.8
14.1A	0.684	38.7	0.799	21.2

2. Device Structure and Fabrication

Figure 1 shows the schematic of ABC silicon wafer solar cell fabricated at ANU. The cell substrate has a thickness of approximately 200 µm. The front surface of the cell, featuring the texturing together with a stack of high-quality thermally grown passivation oxide (SiO_2 = ~20-25 nm) and PECVD nitride (SiN_x = ~55 nm), improves light trapping and provides effective surface passivation. The presence of light phosphorus diffusion further minimises the front surface recombination. The rear surface features interdigitated patterns of n^+ and p^+ diffusion, both of which are deposited by a stack of SiO_2 and SiN_x; serving the passivation of the rear surface and isolation from the metallised aluminium (Al). The cell has a pitch of 650 µm (i.e. n-diffusion to p-diffusion), covering an approximate fraction of 25% for n-diffusion and 75% for p-diffusion. Metallisation is realised by vacuum-evaporation of Al, which contacts to the diffused regions through point contact holes.

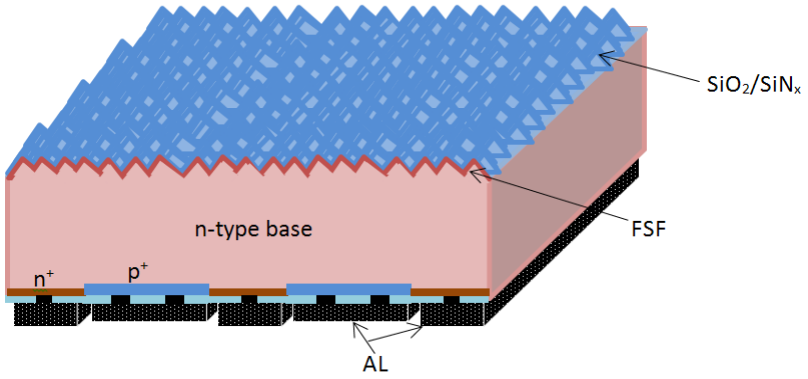

Fig. 1. Cross-sectional device structure of ABC silicon wafer solar cell.

The cell process begins with saw-damage etching the n-type float-zone (FZ) and Czochralski (Cz) <100> silicon wafers with substrate resistivity of 1 Ωcm having 250 micron thick. The saw damage etch (1:10 of HF:HNO_3) thins down the wafer to 200 µm in thickness. Next, the wafers receive standard RCA cleaning, followed by heavy phosphorus diffusion (n^+) having sheet resistance of 40 Ω/□ accompanied by in-situ oxide growth on both front and rear surfaces. A thin LPCVD nitride (~24 nm) is grown conformally on both surfaces (front and rear). Inductively coupled plasma (ICP) etching (80W ICP, 120W RF, 24 seconds) is then used to etch off front LPCVD nitride only, leaving the underlying oxide un-etched. Following the ICP, the wafers undergo 10% HF etch for 1-2 min to remove the front oxide, followed by random pyramid texturing at 85ºC for 60 min. Light phosphorus diffusion (240 Ω/□) is then performed to create FSF. All sacrificial dielectric layers (SiO_2 and SiN_x) are then removed, followed by growing of a thick masking wet-oxide (~ 200 nm) on both sides of cell wafers. Boron diffusion (p^+) windows are then created by lithography means, and exposed n^+ diffusion in p^+ windows are then etched off in TMAH (85°C for 3 min), which removes about 2-3 µm of silicon. Next, the masking oxide is removed and a stack of thermally grown passivation oxide (~20-25 nm) and PECVD nitride anti-reflection coating (ARC) of 55 nm is then deposited on both front and rear. Metallisation then begins creating arrays of lithographically-aligned point contacts (5 µm diameter with 70 µm pitch) on the rear dielectric, followed by vacuum-evaporating the aluminium (Al) as thick as 3 µm. Following the metallisation, lithography is used to transfer interdigitated patterns, followed by etching of Al that separates p- and n-metallisation regions. The cell wafers are then annealed in forming gas environment at 250°C for 30 min.

3. Results and Analysis

Following the fabrication the cell wafers were measured for current-voltage performances by the steady-state light source under one-sun illumination. During the measurement the cell wafers were covered by shadow masks to determine the performance of 16-cm^2 and 13-cm^2 sized ABC cells. Table 2 illustrates the one-sun electrical parameters of 16-cm^2 ABC cells. The best-performed ABC cell made from FZ and Cz wafers is operating at 21.7% with open-circuit voltage higher than 680 mV, short-circuit density close to 40 mA/cm^2 and 80% of FF. As compared to the previously reported best-cell result (Table 1), the cell efficiency is increased by another 0.5% absolute. Detailed analysis on optimisations of FSF, ARC SiN_x, rear diffusion and aligned metal contacts that were implemented in the current cell process are presented on the following pages.

Table 2. One-sun electrical parameters of ABC cells measured using 16-cm^2 aperture mask.

Cell ID	Wafer Type	Resistivity (Ωcm)	Voc (V)	Jsc (mA/cm^2)	FF	Eff (%)	Rsh (kΩcm^2)	Rs-dark (Ωcm^2)	Rs-light (Ωcm^2)
15-6A	FZ	1	0.683	39.3	0.804	21.6	100	0.45	0.62
15-6B	FZ	1	0.685	39.4	0.805	21.7	100	0.45	0.63
15-3A	Cz	5	0.681	40.7	0.768	21.3	27	0.70	

3.1. FSF Optimisation

Lightly doped phosphorus diffusion with sheet resistance of ~190 Ω/□ was used to create FSF in the cells of the old process (Table 1). In the current cell process (this paper), the FSF was further optimised by the addition of drive-in step, resulting with the sheet resistance of 240 Ω/□. Measuring of dark saturation current (J_{oe}), realized by Photoconductance technique to determine the passivation quality of diffused regions, began with preparation of FSF samples (P-type float zone high resistivity (~120 Ω-cm) <100>) with texturing both sides, followed by the process of symmetric phosphorus diffusion and depositing a stack of thin oxide (~20-25 nm) and PECVD nitride (~50-55nm) on both front and rear. PC results show that a further reduction of J_{oe} by 20 fA/cm^2 is achieved through the optimisation of FSF (Table 3). The extraction of J_{oe} from other diffused regions is realised by preparation of samples similar to the process of FSF sample, and measured by the PC technique. Figure 2 illustrates the contribution of J_{oe} from each individual diffused regions of the ABC cell. The contribution of J_{oe} from individual diffused region is deduced by the product of double-sided J_{oe} (obtained through PC technique) and the effective area of the diffused region (i.e. n^+ fingers equate to ~25% of rear surface, p^+ fingers to ~75% of rear surface, n^+ metal contact dots to ~0.1% of the rear surface and p^+ metal contact dots to ~0.4% of the rear surface). Total J_{oe} contribution from all individual diffusion regions in the present work stands at 102 fA/cm^2.

Table 3. PCD results of characterisation samples processed together with cell wafers. J_{oe} represents single-sided value and the measurement of J_{oe} is undertaken at an injection level of 5×10^{15} cm^{-3}. The process of characterising the sample B in the old process is similar to that of the sample A in the current process, except with the heavier front surface diffusion, resulting in sheet resistance of 190 Ω/□.

Cell ID	J_{oe} (fA/cm^2)	Sheet Resistance (Ω/□)
Sample A (current work	35	190
Sample B (previous work)	15	238

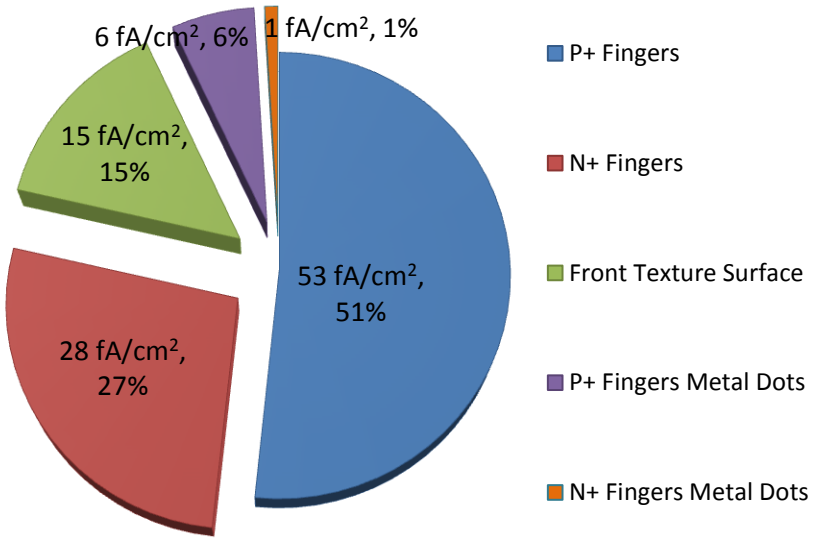

Fig. 2. The breakdown of J_{oe} from individual diffusion regions of the ABC cell shown in Fig. 1. p^+ diffusion has sheet resistance of 58 Ω/□ and n^+ diffusion has 32 Ω/□. The J_{oe} values are measured at an injection level of 5×10^{15} cm^{-3}.

3.2. ARC Layer Improvement

A stack of thermally grown thin SiO_2/PECVD SiN_x serves the purposes of passivation and anti-reflection property in the ABC cells. In the current process, thickness of thermal SiO_2 and PECVD SiN_x were further increased to optimise the front surface reflectance (FSR). The measurement of FSR is realised by spectrophotometer, and Fig. 3 demonstrates the comparison of FSRs of old and current processes. The OPAL 2, published freeware [13, 15], was used to analyse the thickness of dielectric layers. Based on the model, measured FSR of the cell in the current process can be well fitted to 25 nm of SiO_2 and 57 nm of SiN_x, while that in the old process is 22 nm of SiO_2 and 48 nm of SiN_x. The model also demonstrates that the generation current (J_G) is increased by 0.2 mA/cm^2 due to the improved reflectance of the ABC cells (current process).

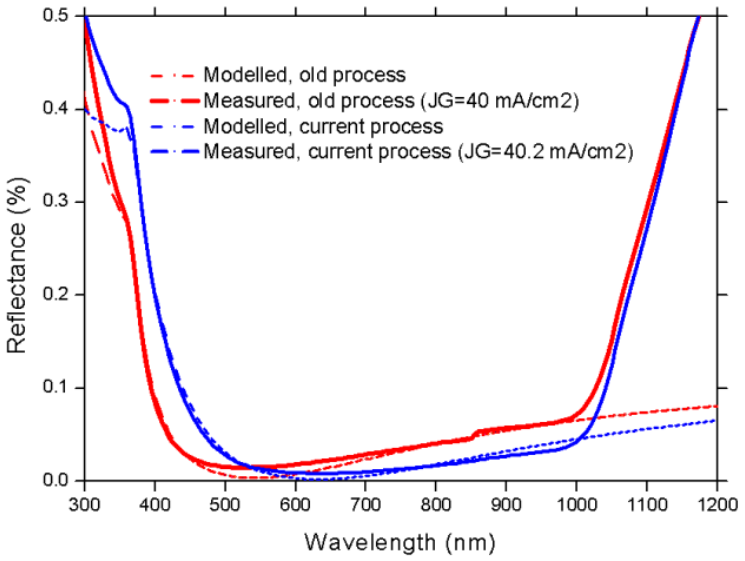

Fig. 3. The analysis of dielectric layer thickness through model-fitting by OPAL 2. J_G stands for current generated, assuming spectrum of AM1.5G and pathlength enhancement of Z = 6 driven by internal reflection. The model uses 20% of planar and 80% of texture (ideal random upright pyramids, with unpolarised normally incident monochromatic light) topography for both FSRs measured.

3.3. Series Resistance Improvement

The total series resistance (R_s) of the champion ABC cell was obtained by curve-fitting the shifted dark JV and illuminated JV, a method described elsewhere [16-18]. According to the curve fit, the R_s value of the best ABC in the current process stands at 0.62 Ωcm^2. When compared to the R_s of the old process, it is lower by 0.08 Ωcm^2 in absolute. The reduction in the R_s could have been attributed by the heavier phosphorus diffusion, resulting in the sheet resistance of 32 Ω/□ (45 Ω/□ in old process) and the photo-lithographically aligned metal contact dots (Fig. 4). The metal contact dots formation by aligned lithographic mean creates defined numbers of metal contacts to every n- and p-diffusion fingers (Fig. 4b), while non-aligned method results in random numbers of contact dots on the fingers (Fig. 4a). The grid resistance and internal series resistance of the ABC cell should have negligible contribution on the overall series resistance, since the thickness of metal (Al, 3 µm) deposited, the device pitch and the substrate resistivity (1 Ωcm) of the cell in the current process are unchanged as compared to the old process.

4. Future Improvements for Increased Cell Performance

In this section, we present further refinements in areas of texturing; front surface field (FSF) passivation; electrical shading loss in terms of cell pitch, bus-bar and base doping; and metallisation that are to be introduced in the development of forthcoming 16-cm^2 ABC cells, aiming for the conversion efficiency > 22% in the very short term.

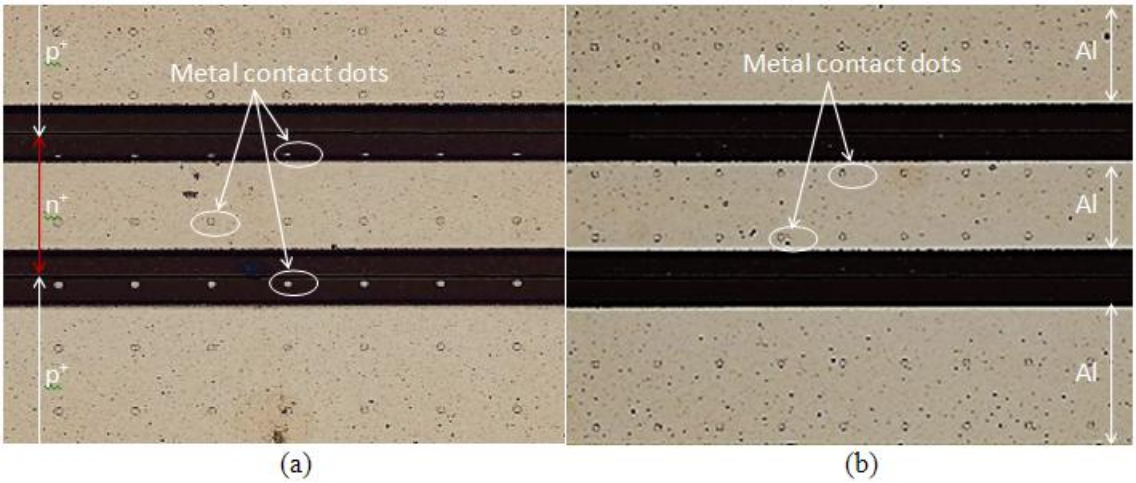

Fig. 4. Images of metal contact on the rear of the ABC cells – (a) metal contacts formed by non-aligned lithographic mean and (b) metal contacts formed by aligned lithographic mean.

4.1. Texturing

In Fig. 3 the curve fitting from the OPAL 2 signifies that the texturing of ABC cells can be improved further. OPAL 2 was also used to predict the performance of J_{sc}, driven by improved texture condition. The results in Table 4 demonstrates that further improving the texturing condition (i.e. reducing the effective planar surfaces) could increase the J_{sc} further by 0.6 mA/cm^2 at maximum. Random pyramidal texturing that we use for the ABC cells development is a TMAH (Tetramethylammonium hydroxide)-based alkaline etch solution. The improvement of the textured condition can be realised by varying the ratio of TMAH content in the texture solution, which is one possible way to improve. The reflectance of bare-silicon sample measured before and after improvement (i.e. varying the ratio of TMAH content) is shown in Fig. 5. The improved texture condition, as verified by the model fit, has resulted in the reduction of reflectance by 1% absolute (300 – 1200 nm).

Table 4. Modelled J_{sc} in relation to texture condition. The model uses the equivalent collection efficiency and reflectance of the ABC cell shown in Figs. 3 and 4. T stands for texture, while P for planar.

Texture Condition	100% T	5% P, 95% T	10% P, 90% T	15% P, 85% T	20% P, 80% T
J_{sc} **(mA/cm^2)**	40.54	40.37	40.20	40.03	39.86

4.2. FSF Passivation

16-cm^2 ABC solar cells having textured front surface with lightly diffused phosphorus and thermally grown SiO_2 have already achieved open-circuit voltage (V_{oc}) as high as 685 mV. To reach an efficiency of 23.5%, V_{oc} higher than 700 mV is required. Since the wafers used for ABC silicon solar cells have very high minority carrier lifetimes and are relatively thin, the main source of recombination is the surfaces. Advanced passivation techniques to further minimise the surface recombination are required. Al_2O_3 is a suitable candidate to passivate the boron emitter in n-type rear-junction silicon solar cells; since it

provides remarkably low recombination rates with surface recombination velocity (SRV) of less than 13 cm/s [19], improved IQE response in the infrared spectrum (600-1200nm) when used as a stack of Al_2O_3 and Si_3N_4 at the rear surface [20] and no presence of parasitic shunting induced by inversion layer [21] as it possesses fixed negative charges. Weber presented that in the case of ABC silicon solar cells the presence of diffused surface (i.e. FSF) at the front surface is not necessarily required for the collection of photogenerated carriers, and a surface with high charge density (without diffusion) offers the superior passivation by repelling carriers from the front surface through the strong electric field [22]. The application of Al_2O_3 passivation on undiffused front surface of n-type ABC solar cells could be well-suited. Figure 6 shows the performances of diffused and undiffused samples passivated with thermal oxide and Al_2O_3. The experiment uses high-resistivity (>120 Ωcm) 100mm n-type FZ <100> 500 micron thick wafers. All samples are random pyramid textured, passivated with SiO_2 or Al_2O_3 (~25 nm) on both front and rear, and forming-gas annealed at 400˚C for 30 min prior to PCD measurement. Both J_{oe} and lifetime are measured at an injection level of 5×10^{15} cm^{-3}.As shown in the figure, the undiffused front surface passivated with Al_2O_3, presenting with very low J_{oe} (10 fA/cm^2, single-side), confirms that front surface recombination can be reduced further though Al_2O_3-assisted field affect passivation, while the cell process is made simpler without the step of FSF diffusion at the front surface.

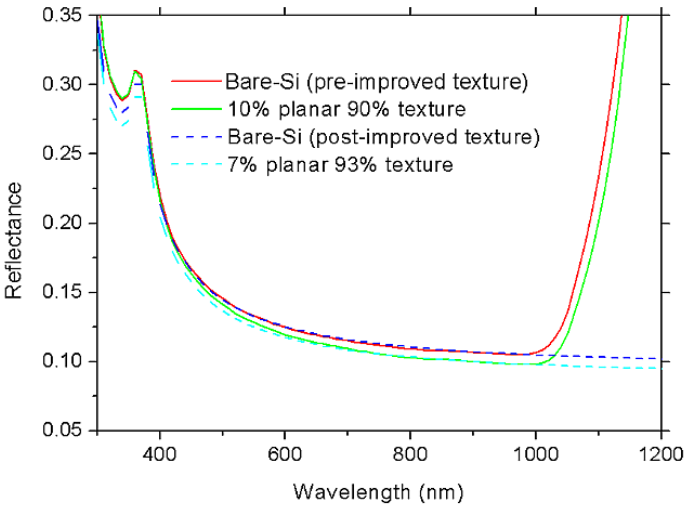

Fig. 5. Reflectance of bare-Si sample measured before and after the improved texturing. Dotted lines are fitted curves by OPAL 2.

4.3. Electrical Shading Loss

Although ABC cells have no optical shading loss given that metal fingers are at the rear of the cells, they are subjected to the electrical shading loss since the minority carriers generated at the base region (i.e. n-bulk) will have to diffuse laterally to the collecting region (i.e. p^+). This often results in increased recombination in the base region, leading to poor collection of minority carrier. In the case of 16-cm^2 ABC cells, the electrical shading loss can be quantified in terms of the cell pitch, rear bus-bar and base doping. A recently published freeware, PC2D featuring a circular-reference spreadsheet method used in conjunction with PC1D, is employed for simulating two-dimensional effects of ABC solar cells based on the cell pitch and substrate resistivity [14].

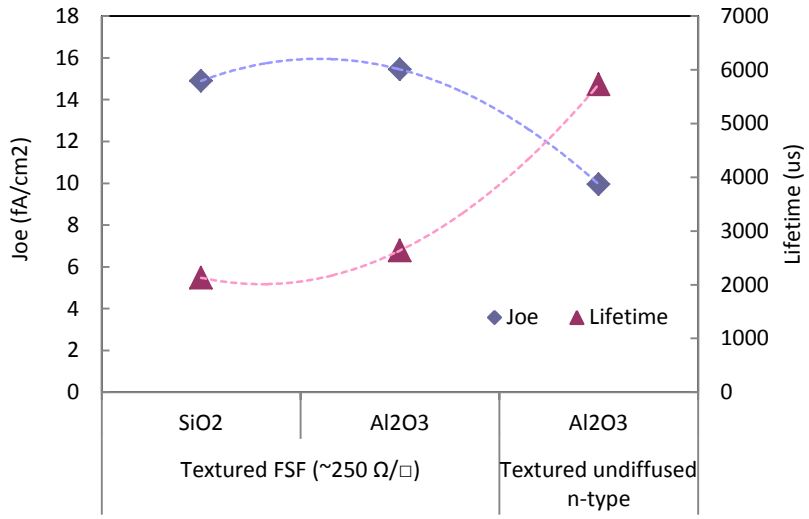

Fig. 6. Saturation current density (J_{oe}) and effective carrier lifetime (T) of samples measured by PCD measurement technique.

4.3.1 Cell Pitch

Increasing the collecting region coverage by reducing the pitch is one way to increase the collection efficiency [23-25]. The simulation makes use of the parameters such as diffusion ratio, recombination values (Fig. 2), measured reflectance (Fig. 3), substrate thickness, type of substrate of the ABC silicon solar cell presented in this paper. From the simulation (Fig. 7), reducing the pitch further increases the ABC cell efficiency.

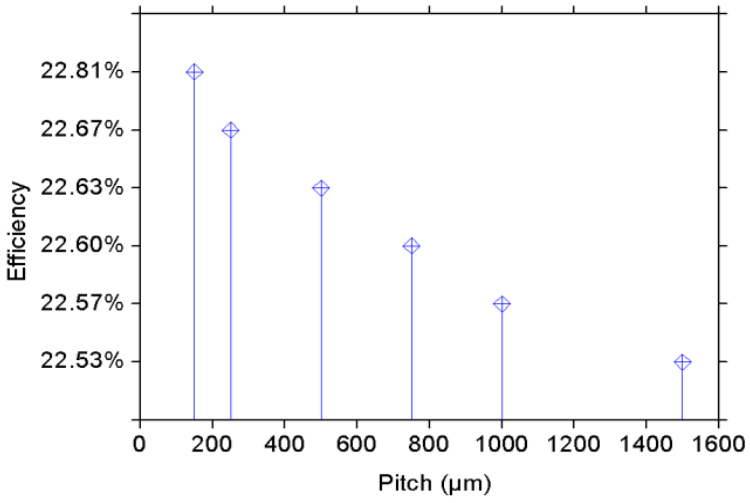

Fig. 7. PC2D simulation for the ABC cell efficiency in relation to the pitch.

4.3.2 Bus-bar

The bus-bars located on the rear side of the 16-cm^2 ABC cells also contribute to inefficient carrier collection capabilities. To quantify that ABC cells were measured for one-sun current-voltage (IV) performance using the shadow masks having areas of 16-cm^2 and 13-cm^2 as shown in Fig. 8. 16-cm^2 sized shadow mask includes the busbars during IV measurement, while 13-cm^2 excludes bus-bars. As observed in Fig. 9, the cell performance is improved by 0.72%, with a major contribution coming from the increase in short-circuit current density, J_{sc}. A slight decrease of open-circuit voltage (V_{oc}) is expected due to the increase of saturation current density (J_o) as a result of J_{sc} increase, while the change in fill factor (*FF*) is insignificant. Reducing the width of the bus-bars will further contribute to the efficiency gain.

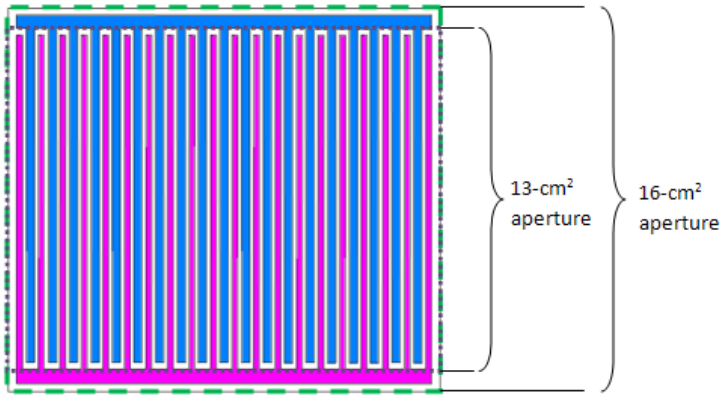

Fig. 8. ABC cells covered with aperture masks having areas of 16 cm^2 and 13 cm^2.

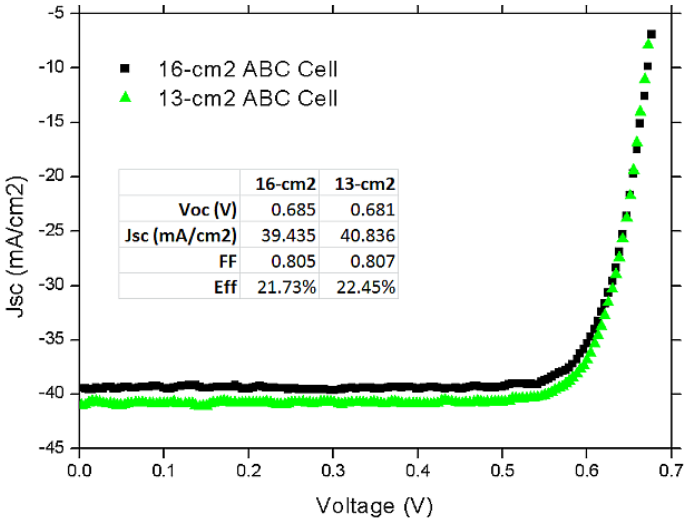

Fig. 9. IV performance of ABC cells measured by 16-cm^2 and 13-cm^2 aperture masks.

4.3.3 Substrate Doping

The simulation, shown in Fig. 10, demonstrates that ABC cells with the substrate resistivity of 1 Ω-cm returns the higher conversion efficiency compared to that of 2.5 and 5 Ω-cm for all cell pitches compared. Of all pitches, the increased in substrate resistivity increases the carrier collection efficiency due to reduced recombination at the front surface and in the bulk, thus leading to increased J_{sc}. However, the reduction in *FF* is also observed, the cause of which could be due to increased internal resistive loss of the photogenerated carriers that have to travel in the bulk to be collected. The change in the V_{oc} is marginal.

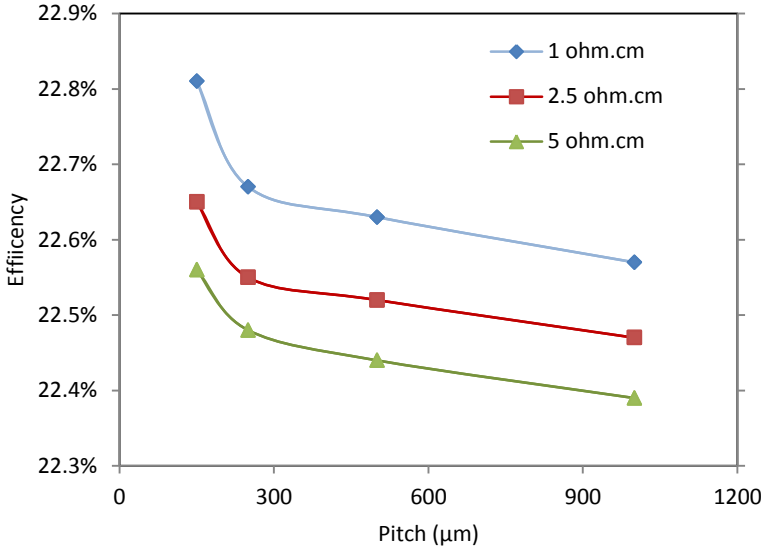

Fig. 10. PC2D simulation for the ABC cell efficiency vs. the base doping on varied cell pitches.

4.4 Metallisation

The ABC cells developed at ANU to date employ vacuum-evaporated aluminium (Al) with a thickness of 3 µm. Replacing the Al with more conductive metal such as silver (Ag) can reduce the finger resistance losses further. The resistivity of Al is about 1.8 times higher than that of Ag. The simulation in Fig. 11 illustrates the power loss (%) in relation to the thickness of the metal – Al or Ag for 16-cm^2 ABC cells with 650 µm pitch. For 16-cm^2 cells 3 micron of Ag is sufficient to reduce less than 1% of power loss induced by grid resistance. Silver electroplating is the feasible method of achieving large thicknesses of Ag.

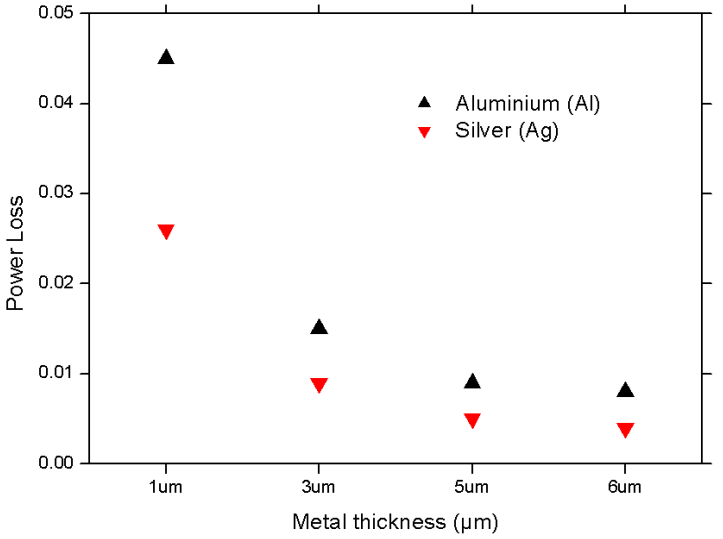

Fig. 11. Modelled ABC cell power loss for the type of metal (Al or Ag) used.

5. Conclusion

The continued development of ABC cells with further optimisations on FSF, ARC layer and phosphorus diffusion coupled with aligned metal contacts at ANU have resulted in further increase of conversion efficiency by 0.5% absolute. Optimisations of FSF, ARC layer and phosphorus diffusion with aligned metal contacts resulted in reduction of front surface J_{oe} by 22 fA/cm^2, reflectance by 4% from 300 nm to 1200 nm wavelength and overall series resistance by 0.08 Ωcm^2. When measured with shadow masks for current-voltage performance, the best cell performs at 22.5% (13-cm^2, FZ substrate, without bus-bars), 21.7% (16-cm^2, FZ substrate, with bus-bars) and 21.3% (16-cm^2, Cz substrate, with bus-bars). Further improvement items - targeting for 22% and beyond of conversion efficiency for 16-cm^2 ABC cells in the immediate future - include improved texturing; front surface improvement by removal of light phosphorus diffusion and passivation by Al_2O_3; improvement on electrical shading loss in areas of reducing the device pitch, selecting the appropriate bulk resistivity and reducing the bus-bar width; and minimising grid resistance by replacing Al with more conductive Ag, realised by electrolyte plating.

Acknowledgements

Funding of this work by Trina Solar is acknowledged. The Solar Energy Research Institute of Singapore (SERIS) is sponsored by the National University of Singapore and Singapore's National Research Foundation through the Singapore Economic Development Board.

References

[1] *Trina Solar Limited, Press release, Trina Solar and SERIS to develop high efficiency solar cells, http://phx.corporate-ir.net/phoenix.zhtml?c=206405&p=irol-newsArticle&ID=1432729&highlight=, June 2010.*

[2] Lammert MD, Schwartz RJ. The interdigitated back contact solar cell: a silicon solar cell for use in concentrated sunlight. *IEEE Trans. Electron Dev. ED* 1977; **24**:337–42.

[3] Schwartz RJ, Lammert MD. Silicon solar cells for high concentration applications. Presented at the *Proc. IEEE International Electron Devices Meeting*, Washington DC, 1975.

[4] Garner CM, Nasby RD, Sexton FW. An interdigitated back contact solar cell with high-current collection. *IEEE Electron Dev. Lett. EDL* 1980; **1**:256-8.

[5] Garner CM, Nasby RD, Sexton FW, Rodriquez JL, Norwoord DP. An interdigitated back contact solar cell with high-current collection. *Proc. 15th IEEE Photovoltaic Specialists Conf.*, Orlando; 1980, pp. 1349-52.

[6] Swanson RM, Beckwith AK, Crane RA, Eades WD, Kwark YH, Sinton RA. Point-contact silicon solar cells. *IEEE Transactions on Electron Devices* 1984; **31**:661-4.

[7] Swanson RM. Point-contact solar cells: theory and modelling. *Proc. 18th IEEE Photovoltaic Specialists Conf.*, Las Vegas, 1985, pp. 604-640.

[8] Cousins PJ, Smith DD, Luan HC, Manning J, Dennis TD, Waldhauer A, Wilson KE, Harley G, Mulligan WP. Generation 3: Improved performance at lower cost. *Proc. Photovoltaic Specialists Conf.*, San Diego, 2010, pp. 275-278.

[9] Smith DD, Cousins PJ, Masad A, Waldhauer A, Westerberg S, Johnson M *et al.* Generation III high efficiency lower cost technology: Transition to full scale manufacturing. *Proc. 38th IEEE Photovoltaic Specialists Conference 2012*, pp. 001594-001597.

[10] Zin N, Blakers A, Franklin E, Kho T, McIntosh K, Wong J *et. al.* Progress in the development of all-back-contacted silicon solar cells. *Energy Procedia* 2012; **25**:1-9.

[11] Zin N, Blakers A, McIntosh K, Franklin E, Kho T, Wong J, Mueller T, Aberle AG, Feng Z, Huang Q. 19% Efficient N-type all-back-contact silicon wafer solar cells with planar front surface. Presented at the 49th AUSES Conference 2011, Sydney, Australia, 2011.

[12] Zin N, Blakers A, Franklin E, Kho T, Chern K, McIntosh K, Wong J, Mueller T, Aberle AG, Yang Y, Zhang X, Feng Z, Huang Q. Laser-assisted shunt removal on high efficiency silicon solar cells. *Proc. 27th European Photovoltaic Solar Energy Conf.*, Frankfurt, Germany, 2012, pp. 552-556.

[13] McIntosh KR, Baker-Finch SC. OPAL 2: Rapid optical simulation of silicon solar cells. *Proc. 38th IEEE Photovoltaic Specialists Conf.*, Austin, Texas, 2012.

[14] Basore PA, Cabanas-Holmen K. PC2D: A circular-reference spreadsheet solar cell device simulator. *IEEE Journal of Photovoltaics* 2011; **1**:72-7.

[15] Available: www.pvlighthouse.com.au

[16] Aberle AG, Wenham SR, Green MA. A new method for accurate measurements of the lumped series resistance of solar cells. *Proc. 23rd IEEE Photovoltaic Specialists Conf., 1993;* pp. 133-139.

[17] Dicker J. Dissertation Thesis, University of Konstanz, 2003.

[18] Rohatgi R, Davis JR, Hopkins RH, Rai-Choudhury P, McMullin PG, McCormick JR. Effect of titanium, copper and iron on silicon solar cells. *Solid-State Electronics* 1980; **23**: 415-22.

[19] Hoex B, Heil SBS, Langereis E, van de Sanden MCM, Kessels WMM. Ultralow surface recombination of c-Si substrates passivated by plasma-assisted atomic layer deposited Al_2O_3. *Applied Physics Letters* 2006;**89**:042112.

[20] Chang WL, Sun WC, Lin CH, Lan CW. High performance monocrystalline silicon solar cells by using rear surface passivation of Al_2O_3/SiN_x stacks structure. *Proc. 23rd European Photovoltaic Solar Energy Conf.*, Valencia, Spain, 2008, pp.1349-1351.

[21] Schmidt J, Merkle A, Brendel R, Hoex B, van de Sanden MCM, Kessels WMM. Surface passivation of high-efficiency silicon solar cells by atomic-layer-deposited Al_2O_3. *Progress in Photovoltaics: Research and Applications* 2008; **16**:461-6.

[22] Weber KJ, Jin H, Zhang C, Nursam N, Jellett WE, McIntosh KR. Surface passivation using dielectric films: how much charge is enough? *Proc. 24th European Photovoltaic Solar Energy Conf.,* Hamburg, Germany, 2009, pp.534-537.

[23] De Ceuster D, Cousins P, Rose D, Vicente D, Tipones P, Mulligan W. Low cost, high volume production of > 22% efficiency silicon solar cells. *Proc. 22nd Photovoltaic Solar Energy Conf.*, Milano, Italy 2007, pp. 816–819.

[24] Hermle M, Granek F, Schultz-Wittmann O, Glunz SW. Shading effects in back-junction back-contacted silicon solar cells. *Proc. 33rd IEEE Photovoltaic Specialists Conf.*, San Diego, USA, 2008, pp. 1-4.

[25] Reichel C, Granek F, Hermle M, Glunz SW. Back-contacted back-junction n-type silicon solar cells featuring an insulating thin film for decoupling charge carrier collection and metallization geometry. *Progress in Photovoltaics: Research and Applications*, 2012; DOI: 10.1002/pip.2204.